Cancer Cell
Article

AID-Dependent Activation of a *MYC* Transgene Induces Multiple Myeloma in a Conditional Mouse Model of Post-Germinal Center Malignancies

Marta Chesi,[1,5,*] Davide F. Robbiani,[2,5,6] Michael Sebag,[1,5] Wee Joo Chng,[1] Maurizio Affer,[1,7] Rodger Tiedemann,[1] Riccardo Valdez,[1] Stephen E. Palmer,[1] Stephanie S. Haas,[1] A. Keith Stewart,[1] Rafael Fonseca,[1] Richard Kremer,[3] Giorgio Cattoretti,[4] and P. Leif Bergsagel[1,*]

[1]Comprehensive Cancer Center, Mayo Clinic Arizona, 13400 East Shea Boulevard, Scottsdale, AZ 85259, USA
[2]Immunology Program, Weill Medical College and Graduate School of Medical Sciences of Cornell University, 1300 York Avenue, New York, NY 10021, USA
[3]Calcium Research Laboratory, McGill University Health Center, 681 Pine Avenue West, Montreal, QC H3A 1A4, Canada
[4]Department of Pathology, School of Medicine, Università degli Studi Milano-Bicocca, Via Cadore 8, 20052 Monza (MI), Italy
[5]These authors contributed equally to this work.
[6]Present address: The Rockefeller University, Laboratory of Molecular Immunology, 1230 York Avenue, New York, NY 10021, USA.
[7]Present address: Molecular Pharmacology and Chemistry Program, Sloan-Kettering Institute-MSKCC, Zuckerman Research Center Building, 415 East 68th Street, New York, NY 10021, USA.
*Correspondence: chesi.marta@mayo.edu (M.C.), bergsagel.leif@mayo.edu (P.L.B.)
DOI 10.1016/j.ccr.2008.01.007

SUMMARY

By misdirecting the activity of Activation-Induced Deaminase (AID) to a conditional *MYC* transgene, we have achieved sporadic, AID-dependent *MYC* activation in germinal center B cells of Vk*MYC mice. Whereas control C57BL/6 mice develop benign monoclonal gammopathy with age, all Vk*MYC mice progress to an indolent multiple myeloma associated with the biological and clinical features highly characteristic of the human disease. Furthermore, antigen-dependent myeloma could be induced by immunization with a T-dependent antigen. Consistent with these findings in mice, more frequent *MYC* rearrangements, elevated levels of MYC mRNA, and *MYC* target genes distinguish human patients with multiple myeloma from individuals with monoclonal gammopathy, implicating a causal role for *MYC* in the progression of monoclonal gammopathy to multiple myeloma.

INTRODUCTION

Cancer cells acquire multiple somatic mutations, with the ultimate tumor phenotype critically dependent upon both the identity of the mutated genes and the precise timing at which these mutations occur during cellular development. Mouse models have sought to faithfully reproduce these events but have been limited by their inability to simultaneously recapitulate the precise timing, tissue specificity, and sporadic nature of the oncogenic events, in which a single cell randomly acquires a mutation that predisposes it to become transformed in a field of normal cells (Rangarajan and Weinberg, 2003). Several conditional expression systems allow the fine control of gene expression in a tissue- and developmental stage-specific manner (e.g., through tet regulation, tamoxifen induction, cre-mediated recombination, or TVA-mediated viral infection); however, none of these are sporadic, as they still produce a lawn of mutant cells (Jonkers and Berns, 2002). In an elegant and unique murine model of sporadic oncogene activation, a mutant K-ras allele is somatically activated by spontaneous recombination in single cells, resulting in the development of both lung tumors and T cell lymphomas (Johnson et al., 2001). However, in this model it has not been

SIGNIFICANCE

Twenty-five years after *MYC* chromosomal translocations were identified in lymphoma, a causative role for *MYC* dysregulation in mature B cell malignancy has finally been established. In previous studies, forced expression of *MYC* in transgenic mice invariably led to pre-germinal center lymphomas. By hijacking the somatic hypermutation machinery, which is implicated in the development of *MYC* chromosomal translocations, we achieved sporadic, AID-dependent activation of *MYC* in the germinal center, uncovering a role for *MYC* in the development of multiple myeloma in mice. Together with the analysis of the expression of *MYC* and *MYC* target genes in human myeloma, these results indicate that *MYC* dysregulation can induce the progression of a benign monoclonal gammopathy to a fully malignant multiple myeloma.

possible to direct the oncogenic event to a given cell type, or a specific time in cellular development.

B cell neoplasms offer a unique advantage in studying tumor development, as their initiating oncogenic events can be related to precisely timed physiologic DNA rearrangements and mutations occurring at the immunoglobulin (Ig) loci. The Ig genes of activated B cells in the germinal center (GC) undergo somatic hypermutation (SHM) and class switch recombination (CSR), resulting in receptors with higher affinity for antigen and enhanced effector function (MacLennan, 1994; McHeyzer-Williams and McHeyzer-Williams, 2005). DNA breaks introduced during these physiologic processes have been postulated to predispose to chromosome translocations in diffuse large B cell lymphoma (DLBCL), Burkitt's lymphoma (BL), multiple myeloma (MM), and mouse plasmacytoma (MPC) (Bergsagel and Kuehl, 2001; Gabrea et al., 1999; Kuppers, 2005). Both SHM and CSR require the activity of Activation-Induced Deaminase (AID), whose enzymatic activity has already been linked to IgH/*MYC* translocations and oncogene mutations (Kotani et al., 2007; Ramiro et al., 2004).

Although *MYC* was identified 25 years ago as the oncogene dysregulated by Ig translocations in BL (Dalla-Favera et al., 1983), MPC (Shen-Ong et al., 1982), and rat immunocytomas (Pear et al., 1988), and by complex translocations in human MM (Avet-Loiseau et al., 2007; Shou et al., 2000), no models have to date convincingly recreated these GC/post-GC disease entities in a mouse. Instead, previous models of forced *MYC* expression mediated by Ig regulatory elements, whose activity initiates in pre-GC B cells, invariably produced pre-GC lymphomas or PC neoplasms lacking significant (>2%) evidence of Ig SHM (Adams et al., 1985; Cheung et al., 2004; Janz, 2006; Kovalchuk et al., 2000; Palomo et al., 1999; Park et al., 2005).

To map sporadic oncogene activation specifically to the GC, we generated transgenic mice in which the activation of *MYC*, under the control of the kappa light chain gene regulatory elements, occurs sporadically through the exploitation of the physiological SHM process in GC B cells. Strikingly, while BL was observed in 2/122 cases only, Vk*MYC mice universally developed post-GC PC tumors that fully recapitulate the biological and clinical features of human MM.

RESULTS

Generation of Matching Vk-MYC and Vk*MYC Mice

We previously generated a vector (Vk-MYC [Robbiani et al., 2005]) with a V-kappa exon splicing in-frame to the coding portion of the genomic locus of human *MYC* (exons 2 and 3), in which the intron-exon structure and polyadenylation signal were maintained, but the first methionine (Met) for initiation of translation was removed. An almost identical vector, Vk*MYC, was generated in which the third codon of the V-kappa exon, TCG, was mutated to a stop codon TAG (Figure 1A). In this Vk*MYC construct, transcription was predicted to occur as in the Vk-MYC vector; however, translation would prematurely abort because of the engineered stop codon, and MYC protein would not be expressed. This stop codon created a DGYW motif that represents a known preferential target sequence for SHM (Rogozin and Diaz, 2004). We hypothesized that in B cells undergoing SHM the same mechanism would also introduce mutations in the transgenic locus, which contains all of the IgK light chain regulatory elements required for targeting by SHM (Betz et al., 1994; Papavasiliou and Schatz, 2000), and sporadically revert the stop codon allowing activation of MYC translation. Transfection experiments in 293T cells confirmed that translation of MYC was completely aborted in the presence of the engineered stop codon and did not initiate from downstream AUG (Figure 1B and Figure S1). Vk*MYC mice were generated by microinjection into C57BL/6 oocytes, and two independent founders were obtained, MYC11 and -24, with 20 and 8 copies of the transgene, respectively (Figure 1C). The kappa promoter and enhancers are active in B cells, beginning at the pro-B stage, but their activity strongly increases with plasma cell (PC) differentiation (Fulton and Van Ness, 1993). Among multiple tissues analyzed, transgenic mRNA expression was detectable only in spleen and bone marrow (BM) and was markedly upregulated upon LPS stimulation to induce PC differentiation (Figure 1D and Figure S2).

Vk*MYC Mice Develop Monoclonal PC Expansion

Constitutive *MYC* expression in early B cells of Vk-MYC mice led to a very aggressive pro-B lymphoma, consistent with the reported phenotype of the Eμ-myc transgenic mice (Adams et al., 1985; Robbiani et al., 2005). Introduction of an engineered stop codon in Vk*MYC ORF completely abolished this phenotype. The two lines of Vk*MYC mice (-11 and -24) behaved identically. At a young age their phenotype was indistinguishable from that of WT littermates (data not shown). With age, however, 100% of the 122 mice analyzed developed a slowly progressive monoclonal expansion of PCs restricted to the BM, reminiscent of human MM (Kuehl and Bergsagel, 2002). IHC staining of BM sections from aged Vk*MYC, but not wild-type (WT), mice showed multiple foci of PCs in which all the CD138-positive PCs are stained with nuclear MYC, indicating activation of the transgene (Figure 2A). PCs in Vk*MYC mice, as in human MM and in contrast to MPC, were mainly not proliferative, with only a minority costaining with $CD138^+$ and $Ki67^+$(Figure 2A, bottom panel). This is not unexpected, despite the fact that *MYC* expression has been often associated with strong proliferative activity: quiescent mantle zone and marginal zone B cells, but not proliferating GC cells, express MYC message (Klein et al., 2003) as well as MYC protein in a subset of human marginal zone cells with a memory phenotype (G.C., unpublished data). Flow cytometry (FCM) on BM and secondary lymphoid organs demonstrated that Vk*MYC mice accumulate terminally differentiated PCs ($CD138^+B220^-$) exclusively in the BM and not in spleen or lymph nodes (Figure 2B). On average the BM PC content by FCM was 12%, with a range of 2%–62%, and approximately 80% of necropsied mice had more then 5% BM PCs.

A feature of MM and other PC neoplasia is the secretion of a large amount of monoclonal antibodies that can be detected in the serum as a distinct band (M-spike) by Serum Protein Electrophoresis (SPEP) (Longsworth et al., 1939). M-spikes were detectable starting at 20 weeks of age in Vk*MYC mice, with their intensity progressing over time, often surpassing that of albumin (Figures 2C and 2D). In most of the mice the PC expansion was monoclonal: out of 85 mice with M-spikes, 70% had a single sharp monoclonal spike, 16% had two, 6% had three, and 8%

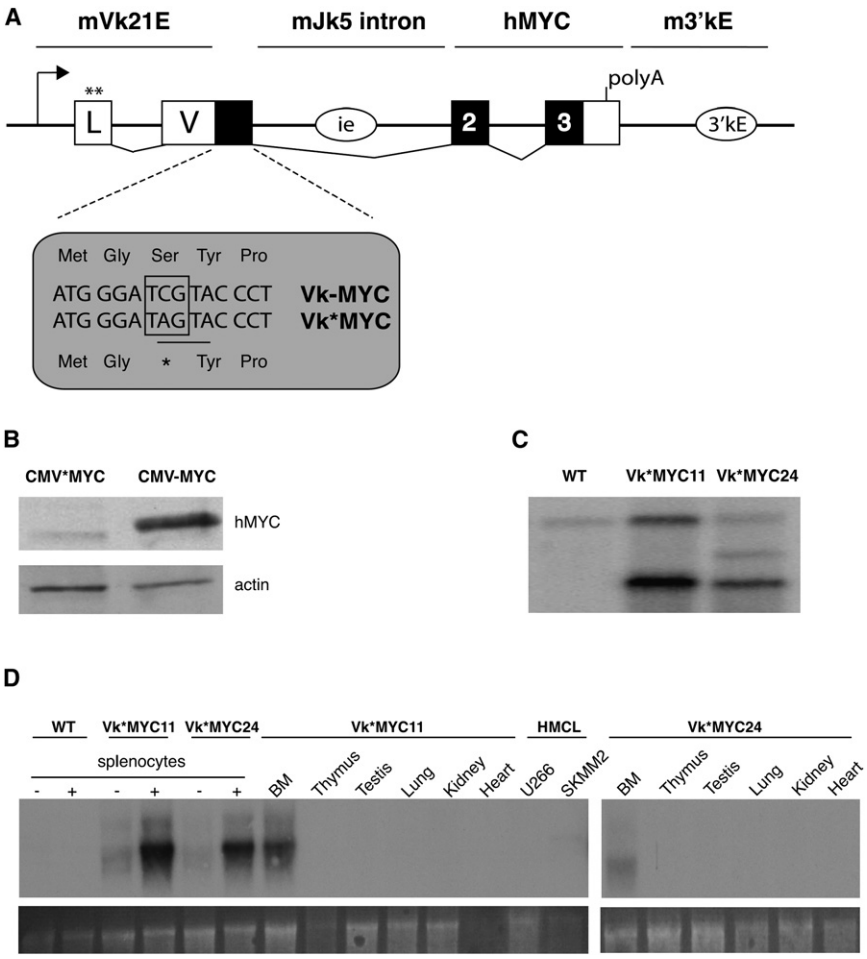

Figure 1. Generation and Regulation of Matching Vk- and Vk*MYC Mice

(A) Schematic representation of the Vk-MYC and Vk*MYC vectors. Displayed is a rearranged Vk21 gene in which the Jk5 exon has been replaced by a short coding exon containing a Kozak ATG, and the Ck region has been replaced by a genomic portion of human MYC (exons 2 and 3). Transcription initiates at the Vk21E proximal promoter (arrow), extends to the leader (L) and Vk (V) exons, splices in frame to hMYC, and terminates at the endogenous polyA signal (shown). Open and black boxes represent noncoding and coding exons, respectively, including *MYC* exons 2 and −3. Diagram is not drawn to scale. Asterisks show ATG codons in the leader (L) exon mutated into ACG to avoid premature initiation of translation. The spatial configuration of the Vk locus has been maintained, and the open circles indicate the two regulatory regions: intronic enhancer (ie) and 3′ kappa enhancer (3′kE). In the ORF closeup panel is shown the nucleotide and amino acid sequence of the first coding exon: the initiation of translation ATG; the TCG > TAG mutated stop codon is boxed, and the DGYW (AGTA) nucleotide sequence, hot spot for SHM, is underlined.

(B) Only CMV but not CMV* constructs express a transgenic MYC protein. 293T cells have been transfected with CMV*- and CMV-MYC constructs, in which the Vk promoter has been replaced by the CMV promoter active in 293T. Total proteins have been analyzed by western blot for human MYC (upper) and β-actin (lower). The lower bands in the MYC blot represent the endogenous MYC protein expressed by 293T cells.

(C) Southern blot on tail DNA from Vk*MYC founders identify 20 and 8 transgene copies in Vk*MYC11 and -24, respectively (lower bands). Top bands represent the endogenous 3′kE locus. The transgene integration site is detected in the Vk*MYC24 founder (middle band).

(D) Transgenic mRNA expression in Vk*MYC mice. Splenocytes from 6- to 8-week-old WT and Vk*MYC mice have been assayed on day 0 (−) or after culturing for 4 days in the presence of LPS (+) to induce PC differentiation. Total RNA from various transgenic tissues was isolated and probed for human MYC. As positive and negative controls, RNA from human myeloma cell lines with (SKMM2) or without (U266) *MYC* rearrangements was assayed. As a loading control, the 28S rRNA is shown in the lower panel.

had multiple spikes. By 50 weeks, 80% of Vk*MYC and only 25% of WT mice had M-spikes. Furthermore, by 80 weeks, although 70% of WT mice had developed small M-spikes as expected (Radl and Hollander, 1974; van den Akker et al., 1988), they secreted five times less IgG than age-matched Vk*MYC mice, as measured by ELISA (median serum IgG 3.25 versus 15.33 g/l) (Figure 2E). Further isotype-specific ELISA experiments demonstrated that the most commonly elevated Ig isotypes in the serum of 70-week-old Vk*MYC mice are IgG1 (median 9.1 g/l versus 0.49 in WT mice) and IgG3 (1.3 versus 0.39) (Figure S3). Two of the mice developed type I cryoglobulinemia, a complication of monoclonal gammopathy (data not shown) (Brouet et al., 1974). The monoclonal gammopathy serves as a useful tumor-specific marker that we used in transplant experiments to assess the reconstitution of the tumor clone in recipient mice. The M-spike could be detected in multiple syngeneic mice serially transplanted with BM mononuclear cells from Vk*MYC mice, starting as early as 4 weeks posttransplant, indicating the tumorigenic nature of these cells (Figure 2F).

PCs in Vk*MYC Mice Have Undergone SHM and Reverted the Engineered Stop Codon

It is well established that long-lived antibody-secreting PCs have been selected in the GC and have acquired somatic mutations of their Ig genes (Jacob et al., 1991; MacLennan, 1991). Single colony sequencing of the VDJ fragment of the heavy chain locus from Vk*MYC CD138-selected tumor PCs showed evidence of SHM in every colony, with a median of 2.6% mutations in the VH gene (Table 1) consistent with the reported range (2%–4.6%) observed following immunization with NP-immune antigen (Driver et al., 2001). As in human MM, we found no evidence of intraclonal heterogeneity, indicating that the tumor cells are no longer subject to ongoing SHM. Interestingly, we found that the number of clones (identified by the specific VH gene used) present in a mouse correlated with the number of Ig spikes observed by SPEP (data not shown). This suggests that activation of the transgene in separate GC cells led to the expansion of independent PC clones. Single colony sequencing of the transgenic locus from CD138-selected Vk*MYC PCs indicated that

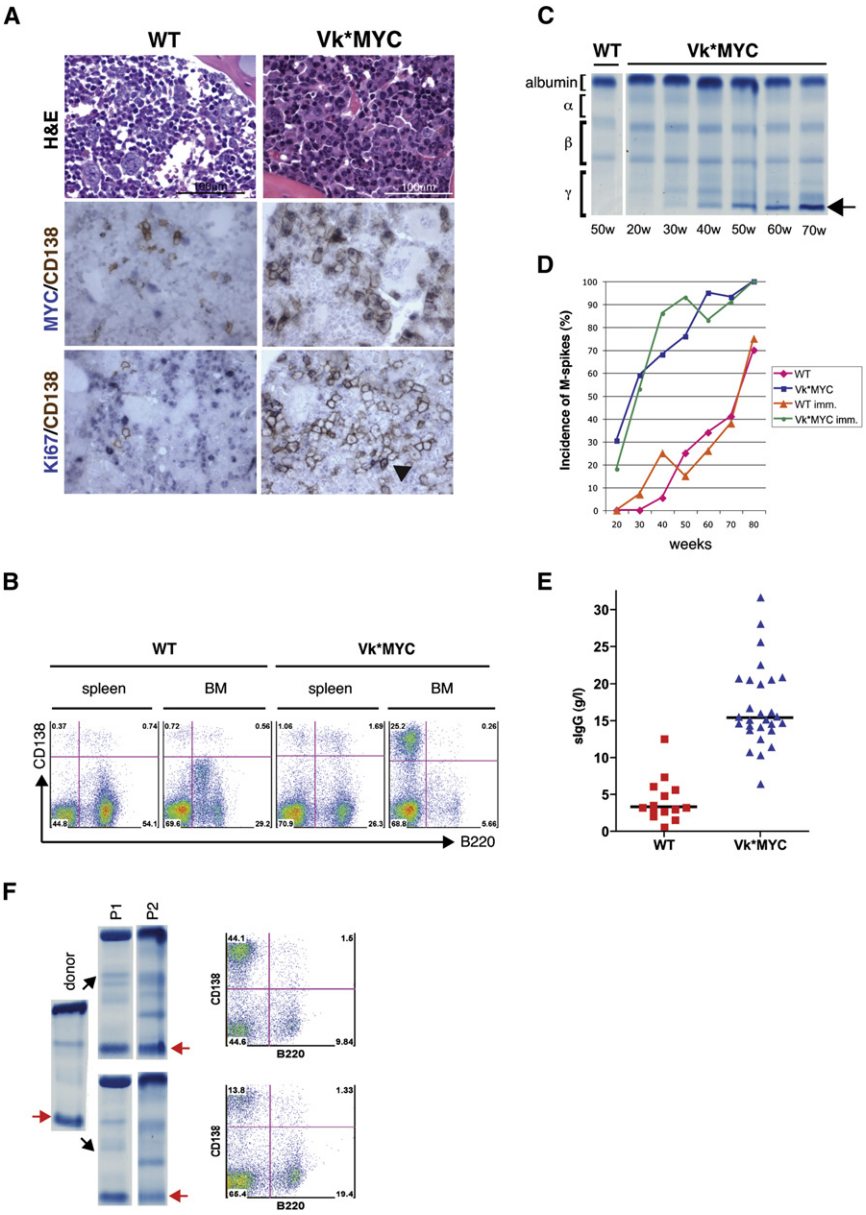

Figure 2. Clonal PC Expansion in Vk*MYC Mice

(A) BM sections from 18-month-old WT and Vk*MYC mice were double stained with H&E, MYC/CD138, and Ki67/CD138. Arrowhead indicates a rare Ki67$^+$ PC. All images are of the same magnification, and scale bar is shown.

(B) Nucleated BM cells from spleen and BM of age-matched WT and Vk*MYC mice were analyzed by FCM. Numbers represent percentage of cells within each gate.

(C) SPEP was performed on a representative WT and a Vk*MYC mouse serially bled at the indicated weeks. The position of the albumin is indicated, and brackets show the different globulin components of the serum. Arrowhead emphasizes M-spike in Vk*MYC mouse.

(D) Incidence of spikes over time (weeks) in a cohort of 40 WT, 60 Vk*MYC, 15 WT immunized, and 15 Vk*MYC-immunized mice.

(E) Total levels of serum IgG (g/l) in 70-week-old WT (n = 14) and Vk*MYC (n = 28) mice, measured by ELISA. Median is 3.22 and 15.33 g/l, respectively ($p < 0.0001$).

(F) Comigration of M-spike (red arrow) detected by SPEP on a donor Vk*MYC mouse and two independent sets of recipient mice following a first (P1) and second (P2) serial transplant of BM mononuclear cells. Flow cytometry detects CD138$^+$B220$^-$ PCs in the BM of P1 recipient mice at the time of second transplant (right). Representative results of three independent sets of transplants are shown.

mutations had targeted the transgenic Vk region (at an average rate of 2.4%, similar to that seen at the endogenous VDJ locus) and reverted the engineered stop codon. Because multiple copies of the transgene are expressed, not every colony showed reversion of the stop codon. However, we conclude that reversion has occurred in every PC since they all expressed *MYC* by IHC (Figure 2A). No mutations were found in the *MYC* exons that are separated from the Vk exon by a 2495 bp Jk5 intron, and therefore are not expected to be targeted by SHM (Pasqualucci et al., 2001). These data indicate that, in addition to the IgH variable region, the SHM machinery had also targeted the transgenic locus leading to the activation of *MYC* expression in post-GC PCs.

Target Organ Damage in Vk*MYC Mice

In addition to the BM localized PC expansion and monoclonal Ig secretion, Vk*MYC mice at necropsy often exhibited target organ damage, which is a defining criterion for human MM (International Myeloma Working Group, 2003). The median hemoglobin concentration at necropsy was significantly lower in Vk*MYC mice than in WT age-matched controls (10.05 g/dl compared to 13.8 g/dl in WT mice), indicating anemia (Figure 3A). In asymptomatic mice, the presence of anemia correlated closely with the presence of a large M-spike on SPEP. Serum Igs could be detected in the tubuli and glomeruli of the kidney from Vk*MYC mice in the form of protein deposition (Figure 3B), a phenomenon associated with myeloma kidney disease. Discrete bone lytic lesions and vertebral collapse, resulting in hindlimb paralysis, have occasionally been detected in Vk*MYC mice (Figure 3C) but are uncommon; nevertheless, bone mineral density analysis (a more objective and quantifiable measure of bone disease) performed on sex- and age-matched mice showed that all Vk*MYC mice suffer from lower bone mineral density (median 0.595 versus 0.727 mg/mm^2, $p = 0.0016$) consistent with diffuse osteoporosis (Figure 3D), the commonest form of bone disease in MM patients. Furthermore, microCT analysis of femurs from a cohort of age- and sex-matched mice demonstrated a significantly decreased trabecular number per unit area, or density in Vk*MYC mice (median 0.523 versus 1.271 #/mm^2, $p = 0.0208$; Figure 3D). Overall, these data clearly

Table 1. Mutational Analysis of VDJ Region and Transgenic Locus in Vk*MYC Mice

Mouse ID	Tumor	VH Gene	DH	JH	No. Mutations at VH	Percent Mutations at VH	No. Clonal Sequences/ Colonies Sequenced	GenBank Accession No.	Engineered Stop Codon Reversion	No. Mutations at tg Locus	Percent Mutations at tg Locus	No. Colonies with Reversion/ Colonies Sequenced
Vk*MYC11 #33BM	MM	J558.53.146	—	—	8	2.9	5/5	EU359464	TAG>TTG	3	1.9	1/14
Vk*MYC24 #37BM	PCT	J558.54.148	DFL16.1	—	8	3.0	4/4	EU359465	TAG>AAG	5	3.1	1/33
Vk*MYC24 #37ASC	PCT	J558.54.148	DFL16.1	—	7	2.6	4/4	EU359466	TAG>AAG	5	3.1	1/16
Vk*MYC24 #31BM	MM	J558.84.190	DFL16.2	JH2	8	3	4/4	EU359467	ND	—	—	—
Vk*MYC24 #1BM	MM	Q52.9.29 Q52.3.8	DST4.3 DFL16.1	JH2 JH2	19 2	7.0 0.7	2/15 9/15	EU359468 EU359479	TAG>TGG	3	1.9	1/8
Vk*MYC11 #37imBM	MM	V186.2	DFL16.1	JH1	13 (W33L)	4.7	7/9	EU359470	ND	—	—	—
Vk*MYC24 #44imBM	PCT	V186.2 V186.2 V186.2 V186.2 V186.2 V186.2	DFL16.1 DFL16.1 DFL16.1 DFL16.1 DFL16.1 DFL16.1	JH2 JH2 JH2 JH2 JH2 JH2	3 (W33L) 2 (W33L) 6 (W33L) 2 (W33L) 9 (W33L) 1 (W33L)	1.1 0.7 2.2 0.7 3.3 0.4	6/13	EU359473 EU359474 EU359475 EU359476 EU359477 EU359478	ND	—	—	—
Vk*MYC11 #11TM	BL	ND	—	—	—	—	—	—	TAG>AAG	2	1.25	1/17
Vk*MYC24 #28TM	BL	Q52.9.29	DSP2.2	JH2	5	1.8	5/15	EU359471	TAG>AAG	5	3.1	4/21
Vk*MYC/ BCL2 #74BM	PCT	J558.53.146	DST4.3	JH2	8	2.9	5/5	EU359472	ND	—	—	—

Results from representative examples are shown. In the first two columns are shown mouse ID (im, NP immunized), tissue analyzed (BM, bone marrow; ASC, ascites; TM, tumor), and the phenotype (MM, multiple myeloma; PCT, plasmacytoma; BL, Burkitt's lymphoma). The identity of the VH, DH, and JH genes, the number of mutations/sequence within the VH gene, and calculated percentage of mutations were obtained by comparison of IgH VDJ sequence to the mouse germline Ig database using the IgBLAST software. In parentheses is the W to L substitution at position 33 of the VH186.2 gene, hallmark of NP immune response. The number of independent colonies sequenced for each tumor and the GenBank accession number are indicated. The last four columns show results of sequencing analysis of region surrounding the engineered stop codon at the transgenic locus: identification of reversion of the engineered stop codon, total number, and percentage of mutations at the locus.

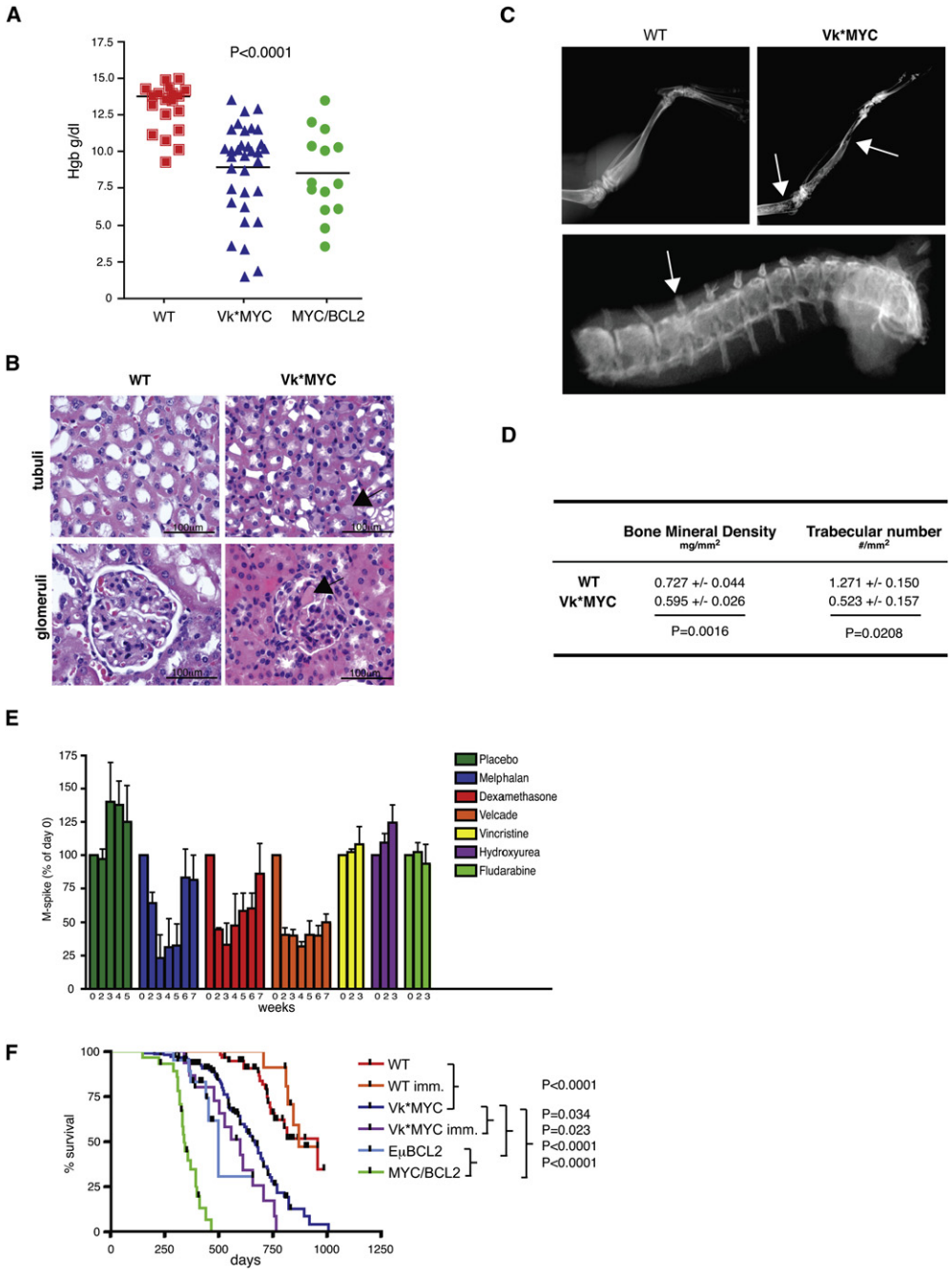

Figure 3. Target Organ Damage in Vk*MYC Mice

(A) Hemoglobin levels in peripheral blood from 20 aged WT (median 13.8 g/dl), 34 Vk*MYC (10.05), and 14 Vk*MYCxEμBCL2 (7.95) mice. The p value is indicated.

(B) Protein deposition in tubuli and glomeruli is evident in H&E-stained kidney sections from Vk*MYC mice, but not in WT control, and an example is highlighted by an arrowhead. Scale bar is shown.

(C) X-ray on spine and femurs from WT and Vk*MYC mice. White arrows point to evident bone lytic lesions and intervertebral spinal compression in a Vk*MYC mouse affected by hindlimb paralysis.

(D) Reduced bone mineral density and trabecular number (by microCT) in Vk*MYC mice (n = 5) compared to age- and sex-matched WT mice (n = 3). ± Standard deviation is indicated.

(E) Response of Vk*MYC mice to clinically active or inactive drugs is shown as variation in M-spike intensity over time after the indicated weeks of treatment, compared to baseline levels (100%). Error bars indicate standard deviation.

(F) Overall survival in days of a cohort of 94 WT, 15 WT immunized, 122 Vk*MYC, 15 Vk*MYC-immunized, 24 EμBCL2, and 25 Vk*MYCxEμBCL2 mice. Median survival in days and p values are shown.

demonstrate that Vk*MYC mice recapitulate both the biological and clinical features of human MM.

Chemotherapy Sensitivity in Vk*MYC Mice Mirrors Clinical Activity in Human MM

To determine the response of Vk*MYC mice to commonly employed chemotherapies in human MM, we selected mice with evidence of significant monoclonal Ig gammopathies (>15 g/l). These mice were treated either with drugs that are known to be clinically active in human MM (Alexanian et al., 1986; Bergsagel et al., 1962; Richardson et al., 2003) or with drugs that have shown little benefit in MM. Profound and statistically significant reductions in M-spike levels (an established surrogate biomarker for MM disease burden) were observed in the mice treated with melphalan, dexamethasone, and bortezomib (Figure 3E). In contrast, mice treated with vehicle alone continued to increase their monoclonal paraproteins during the same treatment period. Despite the occasional complete disappearance of the M-spike on SPEP, responses to all three drugs were transient, as only once cycle of each drug was administered. Vincristine, hydroxyurea, and fludarabine were also given at either well-established doses, or at concentrations limited by myelotoxicity. No activity was observed with these drugs (Figure 3E), consistent with what has been reported in human clinical trials when used as single agents (Davis, 1964; Jackson et al., 1985; Kraut et al., 1990).

Despite developing clinical complications, the majority of Vk*MYC had an indolent disease course, similar to patients with MM, and lived almost 2 years, although with a significant shorter median survival of 661 days, compared to 954 days of WT mice (Figure 3F, compare WT to Vk*MYC, $p < 0.0001$). All of the 122 aged Vk*MYC mice developed a slowly progressive MM that remained confined to the BM in 52% of them (63/122). As in some human MM patients (Allen and Coleman, 1990), 33% of transgenic mice (40/122) progressed to a clonally related, proliferative, extramedullary plasmacytoma (PCT), most commonly $B220^{-}/CD138^{+}$ or occasionally $B220^{+}/CD138^{int}$, that spread to spleen, lymph nodes, and the peritoneal cavity with ascites (Figure S4 and Table 1). The remaining 15% of Vk*MYC mice (18/122), at about 18 months of age developed a spontaneous B cell lymphoma, MYC negative by IHC, clonally unrelated by VDJ sequencing to the MM clone, and similar to the one seen in WT controls (Figure S5 and data not shown). Interestingly, 2/122 transgenic mice developed a very aggressive, highly proliferative, isotype class-switched, somatically mutated, MYC^{+}, $BCL6^{+}$ Burkitt's lymphoma (BL) that invaded multiple organs (kidney, liver, and lung) and infiltrated in the BM, displacing the PCs and causing a remarkably rapid disappearance of the M-spike from the serum (Figure S5). In both these tumors we have identified reversion of the engineered stop codon at the transgenic locus, indicating that activation of *MYC* by SHM can also induce BL (Table 1). Altogether, these results show that sporadic activation of a *MYC* transgene in GCs results in tumors that faithfully recapitulate the human diseases in which *MYC* is dysregulated: BL and MM.

Secondary Events Enable Extramedullary PC Expansion

The survival of long-lived BM PCs is critically dependent on the presence of specific cytokines present at high concentration in the BM microenvironment (Moser et al., 2006; O'Connor et al., 2004). In human MM the growth of malignant PCs is usually restricted to the BM; however, occasional extramedullary dissemination occurs with advanced stages of the disease. Most commonly, clonal PCs in Vk*MYC mice accumulated exclusively in the BM and could not be detected above the normal range in secondary lymphoid organs (Figures 2B and 4A). We hypothesized that, by providing a strong antiapoptotic signal, PCs in Vk*MYC mice could, as in advanced MM, become independent of the survival signal from the BM microenvironment. We crossed Vk*MYC with EμBCL2 mice and monitored them by SPEP for signs of monoclonal PC expansion and tumor development. As previously reported (Strasser et al., 1991), EμBCL2 mice developed a benign polyclonal B cell and PC expansion and remained negative for M-spikes by SPEP (Figure 4), never progressing to a malignant condition during the observation time. In contrast, all 25 double transgenic mice analyzed, starting at 30 weeks of age, developed an aggressive extramedullary monoclonal PCT with infiltration of spleen and lymph nodes (Figure 4A), resulting in a significantly reduced overall survival (median survival 337 days, compared to 661 days in single Vk*MYC transgenic [$p < 0.0001$] and 494 days in single EμBCL2 mice [$p < 0.0001$]) (Figure 3F). Although the aggressive course, localization, and immunophenotype of these tumors resemble those of the iMyc/Bcl-XL mice (Cheung et al., 2004), they differ, as they clearly have a post-GC origin having undergone SHM (Table 1).

Immunization Induced Antigen-Specific MM

We hypothesized that the expression of the transgene in Vk*MYC mice could be induced by the activation of SHM during T cell-dependent antigen response. We thus immunized 15 6- to 8-week-old WT and Vk*MYC mice (without M-spike) with NP-CGG, and following secondary immunization, we found that none of the WT, but 2/8 of the Vk*MYC mice, had developed M-spikes that were specific for NP by eastern blot (Figure 5A). Following their initial and single round of immunization, Vk*MYC mice showed an overall spike incidence (Figure 2D) indistinguishable from that of nonimmunized mice; however, their overall survival was slightly shorter (median 594 versus 661 days, $p = 0.034$) (Figure 3F). This shorter survival was associated with an increased incidence of progression to extramedullary PCT (77% of Vk*MYC-immunized versus 33% in unimmunized mice; Figure 4A), suggesting that the immunization in complete Freund's adjuvant may have increased the pool of *MYC*-expressing cells amenable to the acquisition of secondary mutations. The molecular signature of the NP immune response has been well characterized and includes the use of the Ig-lambda light chain, and the use of VH gene J558 186.2 with selection of the characteristic W to L mutation at position 33 (McHeyzer-Williams et al., 1993; Weiss and Rajewsky, 1990). RT-PCR was performed on total BM cells from 11 Vk*MYC-immunized mice, and overexpression of the Ig lambda gene was detected in three of them (data not shown). VDJ sequence analysis on two of these three mice identified the classic signature (VH J558 186.2 with W33L) of the NP immune response (Table 1). Therefore, our data indicate that at least 3/15 immunized mice developed NP-reactive tumors more than 1 year after immunization. In one case (Vk*MYC24 #44), extensive intraclonal heterogeneity was noted (Table 1).

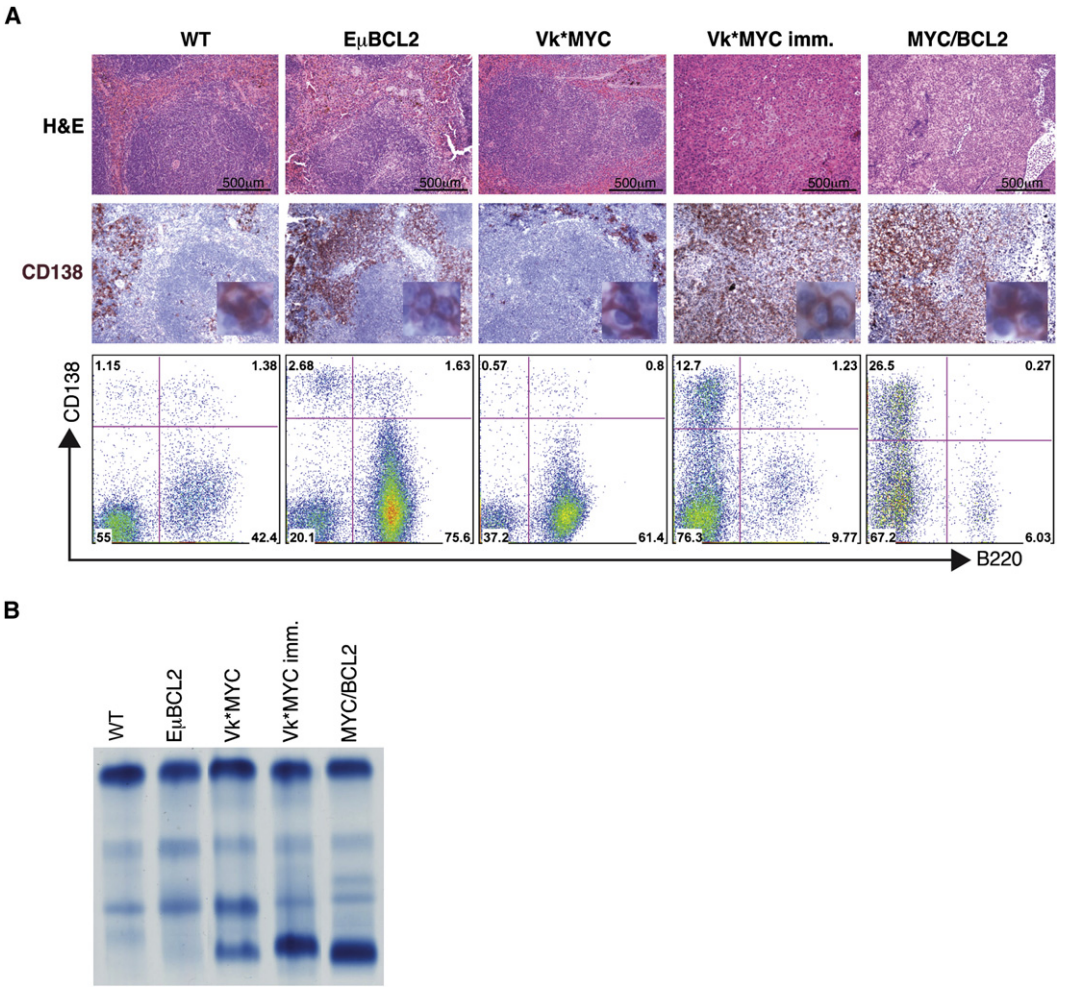

Figure 4. BM-Independent PC Growth in Vk*MYCxEμBCL2 Mice

(A) Spleen sections from aged WT, EμBCL2, Vk*MYC, Vk*MYC-immunized, and Vk*MYCxEμBCL2 mice were stained with anti-CD138 antibody to identify PCs. In the lower panel is shown flow cytometric analysis on the same tissues. Numbers represent cell percentage within each gate. All images are of the same magnification, and scale bar is shown. A zoomed-in insert of $CD138^+$ PCs is shown.

(B) SPEP identified pronounced M-spikes in Vk*MYC, Vk*MYC-immunized, and Vk*MYCxEμBCL2 mice, but not in WT or EμBCL2.

AID Is Required for the Development of MM in Vk*MYC Mice

AID has been identified as a key enzyme required for the SHM process, as B cells from AID knockout mice fail to acquire SHM (Muramatsu et al., 2000). We crossed Vk*MYC mice with AID^{null} mice to test if SHM was responsible for the activation of the transgene observed in the Vk*MYC mice and for MM development. A cohort of 50-week-old sibling AID^{null} (16 mice) Vk*MYCxAID^{het} (17 mice) and Vk*MYCxAID^{null} (18 mice) were bled and the sera analyzed by SPEP. Similar to Vk*MYC mice, 1-year-old Vk*MYCxAID^{het} showed one or more M-spikes; however, none of the Vk*MYCxAID^{null} or AID^{null} mice developed M-spikes (Figure 5B and data not shown). Finally, BM sections from 50-week-old Vk*MYCxAID^{null} mice double stained with MYC- and CD138-specific antibodies showed dramatically fewer PCs and absence of MYC-positive PCs, demonstrating that AID expression and SHM are required for *MYC* activation and PC expansion in Vk*MYC mice (Figure 5C).

Progression from MGUS to MM Is Associated with Activation of the *MYC* Pathway

Given the remarkable resemblance of wild-type C57BL/6 mice to human monoclonal gammopathy of undetermined significance (MGUS) and Vk*MYC mice to human MM, we decided to further assess the potential role of *MYC* activation in human MGUS-to-MM progression. Specifically, we assessed the difference in gene expression profile between MMUS and MM using gene set enrichment analysis (GSEA) (Subramanian et al., 2005). GSEA is a computational method that determines whether an a priori defined set of genes (gene sets that are either experimentally derived from previously published studies, or curated from various databases, and stored in the MSigDB database) shows statistically significant, concordant differences between two biological states (in this case MGUS versus MM). The matching uses statistical methods to determine if genes from the gene sets contained within MSigDB are overrepresented in the genes over- or underexpressed in MGUS compared to MM, and if so whether this could have occurred by chance by using

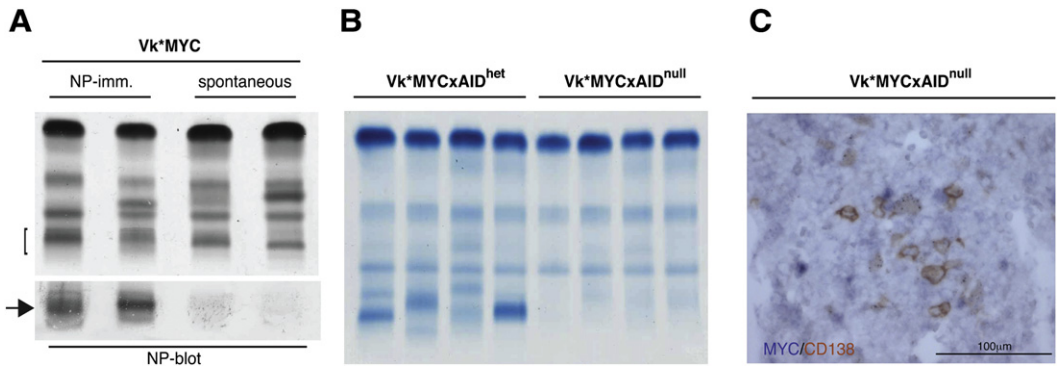

Figure 5. MM in Vk*MYC Mice Are AID Dependent and Can Be Induced by Immunization in an Antigen-Specific Manner

(A) Sera collected from nonimmunized 50-week-old Vk*MYC mice, and from Vk*MYC mice 2 weeks after secondary NP immunization, were analyzed by SPEP (top panel). In parallel, SPEP gel was blotted onto a filter preincubated with NP-biotinylated to identify NP reactive Igs (lower panel). Brackets identify M-spikes; arrowhead points to NP-specific ones.

(B) Sera from 50-week-old Vk*MYCxAID^{het} and Vk*MYCxAID^{null} mice were analyzed by SPEP.

(C) BM section from 50-week-old Vk*MYCxAID^{null} mouse double stained with MYC/CD138-specific antibodies. Only few PCs are detected, all *MYC* negative. Scale bar is shown.

permutation testing. As an internal control, significant enrichment of several relevant MM related gene sets (e.g., genes overexpressed in MM versus amyloidosis, which is biologically similar to MGUS) and of proliferation-associated gene sets, a well-established phenotypic difference between MM and MGUS (Boccadoro et al., 1984; Witzig et al., 1999) was observed using this technique. Strikingly, seven of eight gene sets directly associated with *MYC* activation (from a total of 687 gene sets) were significantly enriched in MM (Figure 6A). Next, we derived a *MYC* gene signature, using a set of recently identified "first neighbors" to *MYC* in a B cell-specific transcriptional network and validated as direct DNA-binding targets of *MYC* by chromatin immunoprecipitation (Basso et al., 2005). In two independent data sets, both *MYC* expression and the MYC signature were not present in normal PCs, rarely weakly present in MGUS, but present in the majority of MM (Figure 6 and Figure S6). This indicates that the elevated MYC mRNA expression is functionally associated with the expected *MYC* transcriptional effect. In other related B cell malignancies, the MYC signature was strongly expressed only in BL, which is characterized by *MYC* translocation to the Ig loci, but was absent in normal peripheral blood B cells, chronic lymphocytic leukemia (CLL), and Waldenstrom macroglobulinemia (WM). In general, the highest *MYC* expression was seen in the samples with strong MYC signature, and both correlate loosely with proliferation (r^2 = 0.3) (Figure 6B). Of interest, some MM samples had *MYC* expression at the impressive levels seen in BL. These may represent MM samples with *MYC* translocations, which have been reported to be present in about 15% of MM (Figure 6C). A MYC index derived from the median expression of genes that form the MYC signature was a more robust discriminator between MM and MGUS ($p < 0.0001$) than *MYC* expression itself, which had more variable expression even in MGUS (Figure 6C). All in all, these data suggest that *MYC* activation is a common and possibly critical event in human MGUS-to-MM progression.

DISCUSSION

A role for AID in tumorigenesis has long been suspected, since mistargeted switch recombination and somatic hypermutation, both processes mediated by AID, are implicated in chromosome translocations or oncogene mutations in B cells (Okazaki et al., 2007). An indirect link between AID and translocations has been established by the finding that AID^{null} IL6 transgenic mice failed to develop IGH/*MYC* translocations (Ramiro et al., 2004). Also, loss of AID in EμMYC mice induced a change in tumor phenotype from B cell to pre-B cell lymphoma, suggesting that AID mutational activity contributes to B cell but not pre-B lymphomas (Kotani et al., 2007). Our data indicate an oncogenic role for AID in post-GC neoplasms. Specifically, we show that in the absence of AID C57BL/6 WT mice fail to develop the post-GC gammopathies that spontaneously occur at high incidence in this strain of mice. In addition, we show that it is possible to direct AID activity to an exogenous substrate (Vk*MYC transgene) to activate an oncogene (*MYC*) and drive post-GC tumorigenesis.

Vk*MYC Construct as a Tool for Modeling Post-GC Malignancies in Mice

MYC has long been associated with GC and post-GC B cell neoplasms, and here we demonstrate the causal role of *MYC* in their development by successfully modeling *MYC*-driven, GC-derived lymphoid proliferation in mice. We report the generation of a mouse model in which activation of an oncogene is both sporadic and initiated by SHM, whose off-target activity has been implicated in oncogene activation in B cell neoplasia. This pathogenetic fidelity results in the phenotypic fidelity of post-GC tumors that recapitulate human disease displaying clinical and therapeutic fidelity.

MYC Activation as a Progression Event from MGUS to MM

Although *MYC* dysregulation has been implicated as a primary event in human BL and a progression event in human MM, out of 122 Vk*MYC mice analyzed, only two developed BL, while they all developed MM. It is possible that the genetic background of Vk*MYC mice may account for their propensity to develop MM. We specifically chose the C57BL/6 mouse strain to generate the Vk- and Vk*MYC transgenic mice because of their high

A

NAME	SIZE	ES	NES	NOM p-val	FDR q-val	RANK
ZHAN_MM_CD138_PR_VS_REST	42	0.82	3.1	0	0	1
SERUM_FIBROBLAST_CELLCYCLE	110	0.63	2.89	0	0	3
SCHUMACHER_MYC_UP	50	0.66	2.65	0	0	16
MENSSEN_MYC_UP	31	0.71	2.49	0	0	26
YU_CMYC_UP	27	0.71	2.4	0	0	36
REN_E2F1_TARGETS	36	0.65	2.36	0	0	42
ZELLER_MYC_UP	23	0.7	2.29	0	0	50
MYC_TARGETS	39	0.6	2.21	0	0	56
CELL_CYCLE	74	0.5	2.14	0	0	66
ZHAN_MULTIPLE_MYELOMA_SUBCLASSES_DIFF	30	0.6	2.08	0	0	77
BRENTANI_CELL_CYCLE	80	0.47	2.03	0	0	86
GOLDRATH_CELLCYCLE	27	0.6	2.03	0	0	87
CELL_CYCLE_KEGG	80	0.46	1.99	0	0	92
ABRAHAM_AL_VS_MM_DN	18	0.63	1.93	0	0	100
COLLER_MYC_UP	17	0.62	1.9	0	0.01	104
ABRAHAM_MM_VS_AL_UP	19	0.6	1.88	0	0.01	113
ZHAN_MM_MOLECULAR_CLASSI_UP	47	0.46	1.8	0	0.01	135
ZHAN_MULTIPLE_MYELOMA_VS_NORMAL_UP	62	0.43	1.75	0	0.02	148
FERNANDEZ_MYC_TARGETS	178	0.33	1.59	0	0.05	198
G1_TO_S_CELL_CYCLE_REACTOME	64	0.36	1.52	0.01	0.07	222
MUNSHI_MM_VS_PCS_UP	76	0.36	1.51	0.01	0.08	227
MUNSHI_MM_UP	65	0.35	1.44	0.03	0.12	250
CELLCYCLEPATHWAY	22	0.41	1.31	0.14	0.22	297
CELL_CYCLE_REGULATOR	24	0.37	1.21	0.2	0.34	346
LEE_MYC_UP	53	0.28	1.13	0.26	0.44	391
LEE_E2F1_UP	60	0.21	0.87	0.7	0.85	564

B

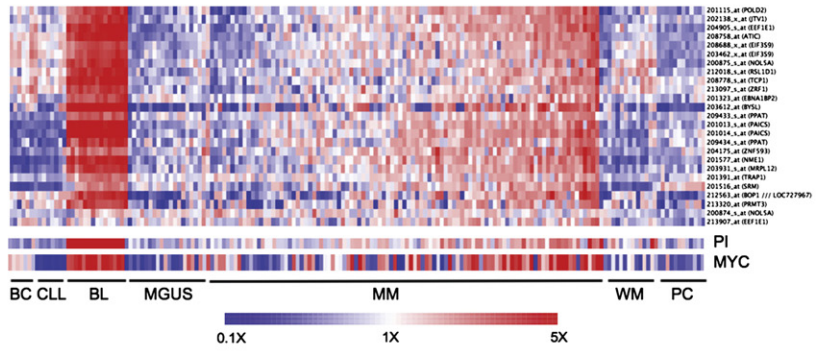

C

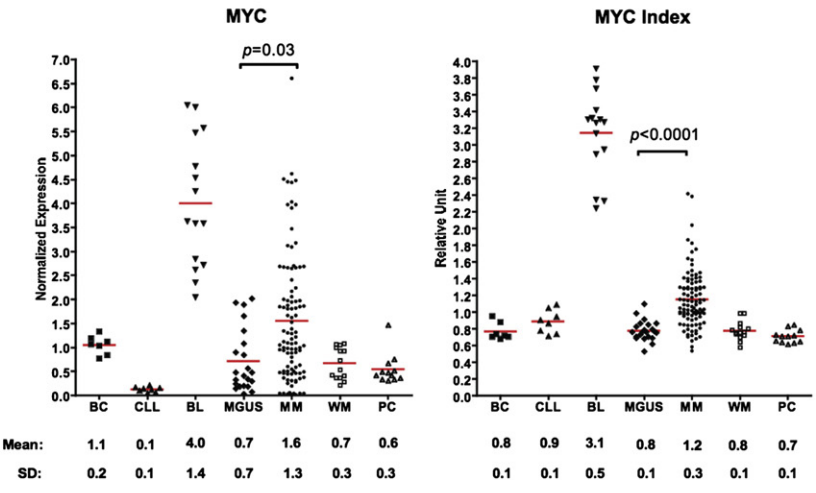

Figure 6. Progression from MGUS to MM Is Associated with Overexpression of *MYC* and *MYC* Target Genes

(A) All the gene sets directly associated with *MYC* activation (highlighted in red), cell cycle, and proliferation (highlighted in blue) and relevant to previous experiment comparing MM to MGUS (highlighted in gray) available in the MSigDB database utilized for GSEA, regardless of whether they are significantly enriched, are selected and presented in the table. These are extracted from the complete list of gene sets (n = 687) used for the analysis (see Table S1). The overall rank of these gene sets in relation to the complete list is also presented. Among these gene sets, those in bold and above the horizontal line are significantly enriched ($p < 0.05$ and $q < 0.05$).

(B) This heatmap represents the expression of genes constituting the MYC signature in normal peripheral blood B cells (BC), chronic lymphocytic leukemia (CLL), Burkitt's lymphoma (BL), MGUS, MM, Waldenstrom macroglobulinemia (WM), and normal plasma cells (PC). The samples are arranged by diagnosis and ascending MYC index. On the heatmap, red indicates overexpression, blue indicates underexpression, and white indicates median expression. The scaling of the heatmap is indicated by the color bar underneath the heatmap.

(C) *MYC* expression and the MYC index are represented as a dot plot according to the different cell/disease type shown in Figure 6B. The horizontal red line represents the mean value. The standard deviation (SD) is indicated.

incidence of spontaneous monoclonal gammopathy with age (van den Akker et al., 1988). We postulate that in this specific strain of mice *MYC* dysregulation may act as secondary genetic event driving the progression of a benign monoclonal gammopathy to a fully malignant MM.

Human MM is preceded by a common premalignant condition called monoclonal gammopathy of undetermined significance (MGUS), which affects 3% of adults over the age of 50 and progresses to fully malignant MM at a rate of 1% per year (Kyle et al., 2006). Although several genetic lesions have been implicated in MM disease progression, the genetic basis for the malignant switch from MGUS to MM remains to be identified. RAS mutations have been identified only rarely in MGUS but are present in 30% of newly diagnosed MM, with an increasing frequency with advanced disease, and have been proposed to induce MGUS-to-MM progression (Rasmussen et al., 2005).

Our results in the Vk*MYC mouse model prompted us to investigate further the role of *MYC* dysregulation in the transition from MGUS to MM in humans. We found that, compared to MGUS, the majority of MM expresses, as expected, higher levels of genes associated with proliferation (Boccadoro et al., 1984; Witzig et al., 1999), but also higher levels of MYC, which can reach in some cases the levels seen in BL, and which correlate with higher levels of known *MYC* target genes (Basso et al., 2005). Although these findings per se do not prove a causative role for *MYC* in the progression of MGUS to MM in

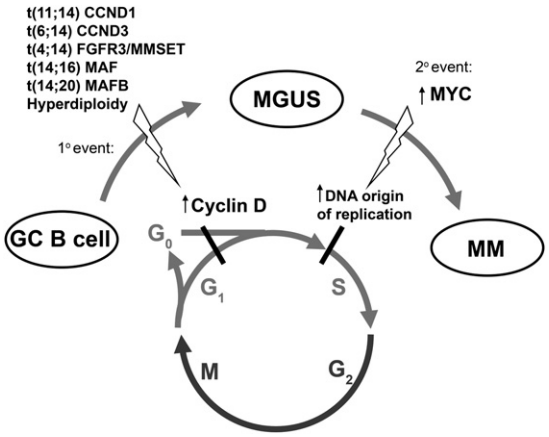

Figure 7. Stepwise Dysregulation of Early Cell Cycle Checkpoints during MGUS and MM Evolution

An early event in MM is overexpression of a cyclin D gene as the result of a primary mutation (translocation or hyperdiploidy). Cyclin D overexpression in PCs presumably enables these cells to autonomously overcome the early G_0G_1 checkpoint, contributing to limited clonal PC expansion (MGUS). Overexpression of *MYC* is one secondary event that may eliminate remaining cell cycle constraints. Significantly, it was recently demonstrated that *MYC* is directly involved in DNA replication, binding and activating DNA replicative origins and regulating progression of cells into S phase (Dominguez-Sola et al., 2007). Therefore, we propose that *MYC* dysregulation is an important progression event between MGUS and MM and mechanistically circumvents cell cycle constraints remaining in cells overexpressing cyclin D by promoting transit into the DNA synthesis S phase through increased DNA replicative origin activity.

human, our results in the Vk*MYC mice, where *MYC* activation in a mouse prone to MGUS leads to MM, suggests that *MYC* is capable of driving the same progression in human. We propose a mechanism in which the primary initiating genetic event, which occurs in a GC B cell (IgH translocation or hyperdiploidy), leads to dysregulation of a cyclin D protein, overcoming the G1 cell cycle checkpoint and resulting in MGUS (Bergsagel et al., 2005). *MYC* activation occurring as a secondary event further increases cell proliferation by promoting transit to S phase through initiation of DNA origin of replication (Dominguez-Sola et al., 2007) (Figure 7).

MYC dysregulation in MM can occur in *cis* by chromosomal rearrangements that are found in 40% of advanced patients by metaphase FISH (Shou et al., 2000), 15% of newly diagnosed MM, but only 3% (2/65) of MGUS by interphase FISH (Avet-Loiseau et al., 2001). Although it is possible that a more comprehensive and detailed analysis of the *MYC* locus may reveal a higher incidence of complex *MYC* translocations for MM patients in whom metaphases are not available, we also postulate that *MYC* activation may occur by dysregulated *trans*-activation through the transcriptional activity of presently uncharacterized factors. In any case, the discovery that *MYC* is implicated in the transition from MGUS to MM, based on our mouse study, re-emphasizes the validity of mouse models not simply as validation tools to assess the contribution of known mutations to cancer, or as drug testing tools, but also as discovery tools that allow the identification of important genetic pathways in human cancer.

Vk*MYC Mice as Model for Human Multiple Myeloma

While it is widely believed that no single mouse model is capable of reproducing all facets of a specific human cancer, the Vk*MYC mice fulfill many of the biologic and genetic criteria of an ideal mouse model, showing a high degree of homology to the clinical phenotype of human MM. First, the Vk*MYC model relies upon a sporadic, yet precisely timed, physiologic mechanism for oncogenic activation, providing a model of tumorigenesis with high penetrance. Reversion of the engineered stop codon SPEP and VDJ sequencing studies indicate that the tumor is indeed clonal, and post-GC in origin, having undergone SHM. Other transgenic mouse models of MM have not convincingly shown evidence of SHM (Table S2). The malignant phenotype of Vk*MYC MM cells is further demonstrated by their successful transplantation into syngeneic recipient mice (Figure 2F). Second, the Vk*MYC mice display histologic and immunophenotypic concordance with human MM and are perfectly suited to the study of the aspects of tumor biology that require an intact and native host-tumor environment. No immunocompetent transgenic mouse model of MM has shown BM-restricted PC growth, but more typically they have displayed an aggressive extramedullary PC proliferation (Table S2). Third, the phenotype in the Vk*MYC mice depends on the activation of *MYC* that, although is not thought to be a primary genetic event in MM, is strongly implicated in the pathogenesis of human MM, where we propose it promotes the progression from MGUS to MM. Further analysis will determine the extent to which the Vk*MYC mice recapitulate the genetic complexity and heterogeneity of the human disease. Fourth, Vk*MYC mice share all of the important clinical features present in human MM. In contrast to existing models, the monoclonal paraproteins in Vk*MYC mice are all isotype class switched and secreted at a level observed in human disease (Table S2). Vk*MYC mice have an indolent course that slowly but invariably leads to end organ damage such as renal dysfunction, bone disease, and anemia. Fifth, while the etiology of *MYC* activation in this model has been engineered, the model nevertheless relies on environmental factors in the form of antigenic stimulation to initiate that activation. Chronic antigenic stimulation has long been implicated in the development of MM, and in rare cases the putative antigen has been identified as a result of exceptionally high titer of reactive Igs against cytomegalovirus, HIV, and streptolysin-O (Kohler et al., 1987; Konrad et al., 1993; Seligmann et al., 1968). Likewise, we were able to generate antigen-specific MM tumors by immunization, suggesting a novel method for the production of monoclonal antibodies. Sixth, the high degree of biologic and phenotypic similarity between the PCs of Vk*MYC mice and human MM cells likely explains the therapeutic fidelity that we have demonstrated in this model. For the preclinical validation of therapeutic agents, it is critical to have a mouse MM model that demonstrates both a response to drugs with known activity in the clinic as well as a lack of response to those with no clinical utility. In conclusion, the Vk*MYC model of MM fulfils all of the above criteria of an ideal mouse model (Table S2) and will be useful for the study of MM cell biology and genetics in a native environment, as well as serve as a powerful tool to predict the utility of novel MM treatment strategies.

EXPERIMENTAL PROCEDURES

For detailed information, please refer to the Supplemental Data.

Mice

All experiments were performed under The Mayo Foundation Institutional Animal Care and Use Committee (IACUC) approval and conformed to all the regulatory standards. The linearized Vk*MYC and Vk-MYC constructs were microinjected into pure C57BL/6J fertilized eggs (SKI/Cornell Transgenic Mouse Core, New York).

For survival studies, mice were aged until they showed evident signs of tumor and/or discomfort and then sacrificed. Sibling control mice were sacrificed at the same time or allowed to age further. Necropsy was performed to assess the presence of phenotypic abnormalities. Statistical analysis was performed on the Prism software (GraphPad Software Inc.); survival curves were generated using the Kaplan-Meyer method and were compared using a log-rank test. EμBCL2 mice in pure C57BL/6 background were purchased from The Jackson Laboratories. AID^{null} mice in pure C57BL/6 background were a gift from Dr. M. Nussenzweig.

Flow Cytometry

The following antibodies were used alone or in combinations on single-cell suspensions: CD3 (17A2), CD19 (1D3), Kappa (187.1), CD43 (S7), B220 (RA3-6B2), IgM (II/41), IgD (11-26c.2a), and CD138 (281-2) (all BD Pharmingen). Data were acquired on a CyanADP (Dako Cytomation) instrument and analyzed with FlowJo software (Tree Star).

Immunizations

Eight- to sixteen-week-old mice (eight Vk*MYC and four WT controls) were immunized intraperitoneally with 50 μg NP-CGG (Biosearch Technologies) emulsified in complete Freund's adjuvant (Sigma) and boosted 6 weeks later with same amount of antigen in incomplete Freund's adjuvant (Sigma).

Gene Expression Cohort

A Mayo cohort of 101 MM, 22 MGUS, 14 Waldenstrom Macroglobulinemia (WM), 7 Chronic Lymphocytic Leukemia (CLL), 6 normal donors of peripheral blood B cells (BC), and 15 normal donors of plasma cells (PC) were included in the study. All patients donated samples following informed consent. The study was approved by the Mayo Foundation Institution Review Board. RNA from purified tumor population was extracted and gene expression profiling performed using the Affymetrix U133A gene chip.

Electronic Availability of the Data

The gene expression data have been previously published (Gene Expression Omnibus [GEO] accession number GSE6477). Another gene expression data set comprised of 22 PC, 43 MGUS, 351 MM, and 44 human myeloma cell lines performed on the U133plus2.0 gene chip was also analyzed (GEO accession numbers GSE2658 and GSE 5900). Burkitt's lymphoma gene expression data generated with the U133A gene chip were extracted from a data set published in GEO (accession number GSE4475).

Supplemental Data

The Supplemental Data include Supplemental Experimental Procedures, six supplemental figures, and two supplemental tables and can be found with this article online at http://www.cancercell.org/cgi/content/full/13/2/167/DC1/.

ACKNOWLEDGMENTS

This work was supported by grants from the National Institute of Health RO1-AG020686 (P.L.B.), RO1-CA83724 (R.F.), RO1-CA129009 (A.K.S.), SPORE P50-CA100707 (R.F. and P.L.B.), P01-CA62242 (R.F.) and funding from the Multiple Myeloma Research Foundation (M.A. and M.S.) and the Fund to Cure Myeloma (P.L.B.). R.F. is a Clinical Investigator of the Damon Runyon Cancer Research Fund. We thank Dr. M. Nussenzweig for discussion and for donating the AID^{null} mice and K. Colon for assistance with mouse bleeding and genotyping. We thank Dr. Herbert Morse for histologic review and Dr. Paul Szabo for assistance with eastern blots. We are grateful to Dr. Freda Stevenson for critical review of the manuscript and to Dr. Mike Kuehl for suggesting a role for *MYC* in the MGUS-to-MM progression in human.

Received: September 11, 2007
Revised: November 27, 2007
Accepted: January 8, 2008
Published: February 4, 2008

REFERENCES

Adams, J.M., Harris, A.W., Pinkert, C.A., Corcoran, L.M., Alexander, W.S., Cory, S., Palmiter, R.D., and Brinster, R.L. (1985). The c-myc oncogene driven by immunoglobulin enhancers induces lymphoid malignancy in transgenic mice. Nature *318*, 533–538.

Alexanian, R., Barlogie, B., and Dixon, D. (1986). High-dose glucocorticoid treatment of resistant myeloma. Ann. Intern. Med. *105*, 8–11.

Allen, S.L., and Coleman, M. (1990). Aggressive phase multiple myeloma: A terminal anaplastic transformation resembling high-grade lymphoma. Cancer Invest. *8*, 417–424.

Avet-Loiseau, H., Gerson, F., Magrangeas, F., Minvielle, S., Harousseau, J.L., and Bataille, R. (2001). Rearrangements of the c-myc oncogene are present in 15% of primary human multiple myeloma tumors. Blood *98*, 3082–3086.

Avet-Loiseau, H., Attal, M., Moreau, P., Charbonnel, C., Garban, F., Hulin, C., Leyvraz, S., Michallet, M., Yakoub-Agha, I., Garderet, L., et al. (2007). Genetic abnormalities and survival in multiple myeloma: The experience of the Intergroupe Francophone du Myelome. Blood *109*, 3489–3495.

Basso, K., Margolin, A.A., Stolovitzky, G., Klein, U., Dalla-Favera, R., and Califano, A. (2005). Reverse engineering of regulatory networks in human B cells. Nat. Genet. *37*, 382–390.

Bergsagel, D.E., Sprague, C.C., Austin, C., and Griffith, K.M. (1962). Evaluation of new chemotherapeutic agents in the treatment of multiple myeloma. IV. L-Phenylalanine mustard (NSC-8806). Cancer Chemother. Rep. *21*, 87–99.

Bergsagel, P.L., and Kuehl, W.M. (2001). Chromosome translocations in multiple myeloma. Oncogene *20*, 5611–5622.

Bergsagel, P.L., Kuehl, W.M., Zhan, F., Sawyer, J., Barlogie, B., and Shaughnessy, J., Jr. (2005). Cyclin D dysregulation: An early and unifying pathogenic event in multiple myeloma. Blood *106*, 296–303.

Betz, A.G., Milstein, C., Gonzalez-Fernandez, A., Pannell, R., Larson, T., and Neuberger, M.S. (1994). Elements regulating somatic hypermutation of an immunoglobulin kappa gene: Critical role for the intron enhancer/matrix attachment region. Cell *77*, 239–248.

Boccadoro, M., Gavarotti, P., Fossati, G., Pileri, A., Marmont, F., Neretto, G., Gallamini, A., Volta, C., Tribalto, M., Testa, M.G., et al. (1984). Low plasma cell 3(H) thymidine incorporation in monoclonal gammopathy of undetermined significance (MGUS), smouldering myeloma and remission phase myeloma: A reliable indicator of patients not requiring therapy. Br. J. Haematol. *58*, 689–696.

Brouet, J.C., Clauvel, J.P., Danon, F., Klein, M., and Seligmann, M. (1974). Biologic and clinical significance of cryoglobulins. A report of 86 cases. Am. J. Med. *57*, 775–788.

Cheung, W.C., Kim, J.S., Linden, M., Peng, L., Van Ness, B., Polakiewicz, R.D., and Janz, S. (2004). Novel targeted deregulation of c-Myc cooperates with Bcl-X(L) to cause plasma cell neoplasms in mice. J. Clin. Invest. *113*, 1763–1773.

Dalla-Favera, R., Martinotti, S., Gallo, R.C., Erikson, J., and Croce, C.M. (1983). Translocation and rearrangements of the c-myc oncogene locus in human undifferentiated B-cell lymphomas. Science *219*, 963–967.

Davis, P. (1964). Phase Ii Studies of hydroxyurea (Nsc-32065) in adults: Multiple myeloma and lymphoma. Cancer Chemother. Rep. *40*, 51–52.

Dominguez-Sola, D., Ying, C.Y., Grandori, C., Ruggiero, L., Chen, B., Li, M., Galloway, D.A., Gu, W., Gautier, J., and Dalla-Favera, R. (2007). Non-transcriptional control of DNA replication by c-Myc. Nature *448*, 445–451.

Driver, D.J., McHeyzer-Williams, L.J., Cool, M., Stetson, D.B., and McHeyzer-Williams, M.G. (2001). Development and maintenance of a $B220^{-}$ memory B cell compartment. J. Immunol. *167*, 1393–1405.

Fulton, R., and Van Ness, B. (1993). Kappa immunoglobulin promoters and enhancers display developmentally controlled interactions. Nucleic Acids Res. *21*, 4941–4947.

Gabrea, A., Bergsagel, P.L., Chesi, M., Shou, Y., and Kuehl, W.M. (1999). Insertion of excised IgH switch sequences causes overexpression of cyclin D1 in a myeloma tumor cell. Mol. Cell *3*, 119–123.

International Myeloma Working Group (2003). Criteria for the classification of monoclonal gammopathies, multiple myeloma and related disorders: A report of the International Myeloma Working Group. Br. J. Haematol. *5*, 749–757.

Jackson, D.V., Case, L.D., Pope, E.K., White, D.R., Spurr, C.L., Richards, F., 2nd, Stuart, J.J., Muss, H.B., Cooper, M.R., Black, W.R., et al. (1985). Single agent vincristine by infusion in refractory multiple myeloma. J. Clin. Oncol. *3*, 1508–1512.

Jacob, J., Kelsoe, G., Rajewsky, K., and Weiss, U. (1991). Intraclonal generation of antibody mutants in germinal centres. Nature *354*, 389–392.

Janz, S. (2006). Myc translocations in B cell and plasma cell neoplasms. DNA Repair (Amst.) *5*, 1213–1224.

Johnson, L., Mercer, K., Greenbaum, D., Bronson, R.T., Crowley, D., Tuveson, D.A., and Jacks, T. (2001). Somatic activation of the K-ras oncogene causes early onset lung cancer in mice. Nature *410*, 1111–1116.

Jonkers, J., and Berns, A. (2002). Conditional mouse models of sporadic cancer. Nat. Rev. Cancer *2*, 251–265.

Klein, U., Tu, Y., Stolovitzky, G.A., Keller, J.L., Haddad, J., Jr., Miljkovic, V., Cattoretti, G., Califano, A., and Dalla-Favera, R. (2003). Transcriptional analysis of the B cell germinal center reaction. Proc. Natl. Acad. Sci. USA *100*, 2639–2644.

Kohler, M., Daus, H., Kohler, C., Schlimmer, P., Wernert, N., and Scheurlen, P.G. (1987). Lymphocytic plasmocytoid lymphoma with a three-banded gammopathy: Reactivity of one of these paraproteins with cytomegalovirus. Blut *54*, 25–32.

Konrad, R.J., Kricka, L.J., Goodman, D.B., Goldman, J., and Silberstein, L.E. (1993). Brief report: Myeloma-associated paraprotein directed against the HIV-1 p24 antigen in an HIV-1-seropositive patient. N. Engl. J. Med. *328*, 1817–1819.

Kotani, A., Kakazu, N., Tsuruyama, T., Okazaki, I.M., Muramatsu, M., Kinoshita, K., Nagaoka, H., Yabe, D., and Honjo, T. (2007). Activation-induced cytidine deaminase (AID) promotes B cell lymphomagenesis in Emu-cmyc transgenic mice. Proc. Natl. Acad. Sci. USA *104*, 1616–1620.

Kovalchuk, A.L., Qi, C.F., Torrey, T.A., Taddesse-Heath, L., Feigenbaum, L., Park, S.S., Gerbitz, A., Klobeck, G., Hoertnagel, K., Polack, A., et al. (2000). Burkitt lymphoma in the mouse. J. Exp. Med. *192*, 1183–1190.

Kraut, E.H., Crowley, J.J., Grever, M.R., Keppen, M.D., Bonnet, J.D., Hynes, H.E., and Salmon, S.E. (1990). Phase II study of fludarabine phosphate in multiple myeloma. A Southwest Oncology Group study. Invest. New Drugs *8*, 199–200.

Kuehl, W.M., and Bergsagel, P.L. (2002). Multiple myeloma: Evolving genetic events and host interactions. Nat. Rev. Cancer *2*, 175–187.

Kuppers, R. (2005). Mechanisms of B-cell lymphoma pathogenesis. Nat. Rev. Cancer *5*, 251–262.

Kyle, R.A., Therneau, T.M., Rajkumar, S.V., Larson, D.R., Plevak, M.F., Offord, J.R., Dispenzieri, A., Katzmann, J.A., and Melton, L.J., 3rd. (2006). Prevalence of monoclonal gammopathy of undetermined significance. N. Engl. J. Med. *354*, 1362–1369.

Longsworth, L., Shedlovsky, T., and MacInnes, D. (1939). Electrophoretic patterns of normal and pathological human blood serum and plasma. J. Exp. Med. *70*, 399–413.

MacLennan, I. (1991). Immunology. The centre of hypermutation. Nature *354*, 352–353.

MacLennan, I.C. (1994). Germinal centers. Annu. Rev. Immunol. *12*, 117–139.

McHeyzer-Williams, M.G., McLean, M.J., Lalor, P.A., and Nossal, G.J. (1993). Antigen-driven B cell differentiation in vivo. J. Exp. Med. *178*, 295–307.

McHeyzer-Williams, L.J., and McHeyzer-Williams, M.G. (2005). Antigen-specific memory B cell development. Annu. Rev. Immunol. *23*, 487–513.

Moser, K., Tokoyoda, K., Radbruch, A., MacLennan, I., and Manz, R.A. (2006). Stromal niches, plasma cell differentiation and survival. Curr. Opin. Immunol. *18*, 265–270.

Muramatsu, M., Kinoshita, K., Fagarasan, S., Yamada, S., Shinkai, Y., and Honjo, T. (2000). Class switch recombination and hypermutation require activation-induced cytidine deaminase (AID), a potential RNA editing enzyme. Cell *102*, 553–563.

O'Connor, B.P., Raman, V.S., Erickson, L.D., Cook, W.J., Weaver, L.K., Ahonen, C., Lin, L.L., Mantchev, G.T., Bram, R.J., and Noelle, R.J. (2004). BCMA is essential for the survival of long-lived bone marrow plasma cells. J. Exp. Med. *199*, 91–98.

Okazaki, I.M., Kotani, A., and Honjo, T. (2007). Role of AID in tumorigenesis. Adv. Immunol. *94*, 245–273.

Palomo, C., Zou, X., Nicholson, I.C., Butzler, C., and Bruggemann, M. (1999). B-cell tumorigenesis in mice carrying a yeast artificial chromosome-based immunoglobulin heavy/c-myc translocus is independent of the heavy chain intron enhancer (Emu). Cancer Res. *59*, 5625–5628.

Papavasiliou, F.N., and Schatz, D.G. (2000). Cell-cycle-regulated DNA double-stranded breaks in somatic hypermutation of immunoglobulin genes. Nature *408*, 216–221.

Park, S.S., Kim, J.S., Tessarollo, L., Owens, J.D., Peng, L., Han, S.S., Tae Chung, S., Torrey, T.A., Cheung, W.C., Polakiewicz, R.D., et al. (2005). Insertion of c-Myc into Igh induces B-cell and plasma-cell neoplasms in mice. Cancer Res. *65*, 1306–1315.

Pasqualucci, L., Neumeister, P., Goossens, T., Nanjangud, G., Chaganti, R.S., Kuppers, R., and Dalla-Favera, R. (2001). Hypermutation of multiple proto-oncogenes in B-cell diffuse large-cell lymphomas. Nature *412*, 341–346.

Pear, W.S., Wahlstrom, G., Nelson, S.F., Axelson, H., Szeles, A., Wiener, F., Bazin, H., Klein, G., and Sumegi, J. (1988). 6;7 chromosomal translocation in spontaneously arising rat immunocytomas: Evidence for c-myc breakpoint clustering and correlation between isotypic expression and the c-myc target. Mol. Cell. Biol. *8*, 441–451.

Radl, J., and Hollander, C.F. (1974). Homogeneous immunoglobulins in sera of mice during aging. J. Immunol. *112*, 2271–2273.

Ramiro, A.R., Jankovic, M., Eisenreich, T., Difilippantonio, S., Chen-Kiang, S., Muramatsu, M., Honjo, T., Nussenzweig, A., and Nussenzweig, M.C. (2004). AID is required for c-myc/IgH chromosome translocations in vivo. Cell *118*, 431–438.

Rangarajan, A., and Weinberg, R.A. (2003). Opinion: Comparative biology of mouse versus human cells: Modelling human cancer in mice. Nat. Rev. Cancer *3*, 952–959.

Rasmussen, T., Kuehl, M., Lodahl, M., Johnsen, H.E., and Dahl, I.M. (2005). Possible roles for activating RAS mutations in the MGUS to MM transition and in the intramedullary to extramedullary transition in some plasma cell tumors. Blood *105*, 317–323.

Richardson, P.G., Barlogie, B., Berenson, J., Singhal, S., Jagannath, S., Irwin, D., Rajkumar, S.V., Srkalovic, G., Alsina, M., Alexanian, R., et al. (2003). A phase 2 study of bortezomib in relapsed, refractory myeloma. N. Engl. J. Med. *348*, 2609–2617.

Robbiani, D.F., Colon, K., Affer, M., Chesi, M., and Bergsagel, P.L. (2005). Maintained rules of development in a mouse B-cell tumor. Leukemia *19*, 1278–1280.

Rogozin, I.B., and Diaz, M. (2004). Cutting edge: DGYW/WRCH is a better predictor of mutability at G:C bases in Ig hypermutation than the widely accepted RGYW/WRCY motif and probably reflects a two-step activation-induced cytidine deaminase-triggered process. J. Immunol. *172*, 3382–3384.

Seligmann, M., Danon, F., Basch, A., and Bernard, J. (1968). IgG myeloma cryoglobulin with antistreptolysin activity. Nature *220*, 711–712.

Shen-Ong, G.L., Keath, E.J., Piccoli, S.P., and Cole, M.D. (1982). Novel myc oncogene RNA from abortive immunoglobulin-gene recombination in mouse plasmacytomas. Cell *31*, 443–452.

Shou, Y., Martelli, M.L., Gabrea, A., Qi, Y., Brents, L.A., Roschke, A., Dewald, G., Kirsch, I.R., Bergsagel, P.L., and Kuehl, W.M. (2000). Diverse karyotypic abnormalities of the c-myc locus associated with c-myc dysregulation and

tumor progression in multiple myeloma. Proc. Natl. Acad. Sci. USA *97*, 228–233.

Strasser, A., Whittingham, S., Vaux, D.L., Bath, M.L., Adams, J.M., Cory, S., and Harris, A.W. (1991). Enforced BCL2 expression in B-lymphoid cells prolongs antibody responses and elicits autoimmune disease. Proc. Natl. Acad. Sci. USA *88*, 8661–8665.

Subramanian, A., Tamayo, P., Mootha, V.K., Mukherjee, S., Ebert, B.L., Gillette, M.A., Paulovich, A., Pomeroy, S.L., Golub, T.R., Lander, E.S., and Mesirov, J.P. (2005). Gene set enrichment analysis: A knowledge-based approach for interpreting genome-wide expression profiles. Proc. Natl. Acad. Sci. USA *102*, 15545–15550.

van den Akker, T.W., de Glopper-van der Veer, E., Radl, J., and Benner, R. (1988). The influence of genetic factors associated with the immunoglobulin heavy chain locus on the development of benign monoclonal gammapathy in ageing IgH-congenic mice. Immunology *65*, 31–35.

Weiss, U., and Rajewsky, K. (1990). The repertoire of somatic antibody mutants accumulating in the memory compartment after primary immunization is restricted through affinity maturation and mirrors that expressed in the secondary response. J. Exp. Med. *172*, 1681–1689.

Witzig, T.E., Timm, M., Larson, D., Therneau, T., and Greipp, P.R. (1999). Measurement of apoptosis and proliferation of bone marrow plasma cells in patients with plasma cell proliferative disorders. Br. J. Haematol. *104*, 131–137.

Accession Numbers

This paper reports sequences that have been deposited in GenBank under the following accession numbers: EU359464, EU359465, EU359466, EU359467, EU359468, EU359470, EU359471, EU359472, EU359473, EU359474, EU359475, EU359476, EU359477, EU359478, and EU359479.